II CONGRESSO NACIONAL DE ENGENHARIA MECÂNICA
II NATIONAL CONGRESS OF MECHANICAL ENGINEERING
12 a 16 de Agosto de 2002 - João Pessoa – PB

INFLUENCE OF TEMPERATURE FIELD ON THE IGNITION OF HYDROGEN-AIR IN SUPERSONIC UNSTEADY MIXING LAYER

Adriana Ferreira de Faria
Uniminas – União Educacional de Minas Gerais
affaria@uniminas.br
Milton Biage
Paulo Lopes Silva Júnior

Abstract. *Fundamental research in supersonic combustion has been conducted in response to the interest in the development of scramjet engine and the scram accelerator. The high speed associated with the supersonic flow implies short residence times for ignition to be effected. This is the major perceived difficulty in the development of scramjet technology. The other hand, an interesting recent theoretical result in the study of high speed chemically reacting mixing layers is that the significant amount of viscous heating can greatly facilitate the reaction rate and thereby the ignition event. The objective of this work is investigate the influence of temperature field effects on the ignition of hydrogen-air in supersonic unsteady mixing layer. In this work the Collocation Spectral Elements Method with Chebyshev polynomials is used for solution of the partial differential equation .*
Key Words: *Combustion, Supersonic Flow, Mixing Layer.*

1. INTRODUCTION

The aim in the development of supersonic combustor is to maximize the amount of heat release with a minimum of total pressure or stream thrust losses. This is a complex problem, which involves knowledge in the area of chemical kinetics, thermodynamics and dynamics of the fluids, besides requesting techniques of precise simulations. To understand the characteristics of the phenomenon of supersonic combustion it is necessary to consider a realistic description of the chemical mechanisms, an analysis of the effect of the viscous dissipation as the source of thermal energy. Recent theoretical studies showed that the ignition can be facilitated by increasing flow speed though the viscous dissipation of the flow kinetic energy to thermal energy. An important recognition which emerged is that while the high flow rate associated with the supersonic flow implies extremely short time residence for the ignition to be affected, the significant amount of viscous heating which takes place in a high sheared mixing layer can greatly facilitate the reaction rate and thereby the ignition event.

Increasing flow velocity of the air stream, the ignition distance first increasing linearly, due to simple residence time considerations. With further increasing in the air stream velocity, the ignition distance subsequently decreases Arrheniusly with the square of the Mach number in response to the significantly enhanced reaction rate due to the extensive amount of viscous heating. It can be defined two regimes of ignition from the critical temperature concept (the temperature which makes reaction rates of the chain branching reaction and the chain terminating reacting are equal, 924.70K for 1atm): high temperature and low temperature regimes. For all practical purposes, the ignition is not possible when the air temperature is lower than the temperature critical, that is in the low temperature regime, even allowing for the case where the viscous heating is important. (Im et al., 1993; Figueira da Silva et al., 1993; Nishioka and Law, 1995, Faria et al., 1998)

The objective of this work is investigate the influence of temperature field effects on the ignition of hydrogen-air. For this purpose, it is accomplished the numerical simulation of H_2 - air flow in the supersonic unsteady mixing layer, with detailed transport and chemical reaction mechanisms and using the conservative form of the complete conservation equations. The chemical and transport properties are calculated by *Chemkin* and the *Transport Package*, respectively. To solve the problem it was used the collocation spectral element method with polynomials of Chebyshev like described in Canuto et al. (1988). This technique presents a high accuracy in the solution of the spatial derivatives, all calculation were made using the Gauss-Lobatto collocation points, with a grid of 121x105.

2. MATHEMATICAL FORMULATION

The problem consist of a fast air stream and a slow hydrogen stream. The origin is located at the downstream edge of the thin splitter plate. The lengths of the domain in the x^* and y^* directions are L_x and $L_{y,}$ respectively, where $-L_x/2 \le x^* \le L_x/2$ and $-L_y/2 \le y^* \le L_y/2$. The symbol * represents a dimensional variables. The variables are placed in dimensionless form using the properties of the free air stream. The mass, momentum, energy and mass fractions dimensionless governing equations are written in vectorial notation, and have the following form:

$$\frac{\partial U}{\partial t} + \frac{L_x}{(\Delta x^*)_i}\frac{\partial E}{\partial x} + \frac{L_x}{(\Delta y^*)_j}\frac{\partial F}{\partial y} = S\ ,\ U = \begin{pmatrix} \rho \\ \rho u \\ \rho v \\ \rho E \\ \rho Y_k \end{pmatrix},\quad S = \begin{pmatrix} 0 \\ 0 \\ 0 \\ 0 \\ w_k \end{pmatrix} \qquad (1, 2, 3)$$

$$E = \begin{pmatrix} \rho u \\ \rho uu + P - \frac{1}{Re_{\delta_0}}\tau_{xx} \\ \rho vu - \frac{1}{Re_{\delta_0}}\tau_{xy} \\ \rho uE + \frac{1}{Pe}q_x + Pu - \frac{1}{Re_{\delta_0}}(\tau_{xx}u + \tau_{xy}v) \\ \rho uY_k + \frac{1}{Re_{\delta_0}\ Sc}J_{k\,x} \end{pmatrix}, F = \begin{pmatrix} \rho v \\ \rho uv - \frac{1}{Re_{\delta_0}}\tau_{xy} \\ \rho vv + P - \frac{1}{Re_{\delta_0}}\tau_{yy} \\ \rho vE + \frac{1}{Pe}q_y + Pv - \frac{1}{Re_{\delta_0}}(\tau_{xy}u + \tau_{yy}v) \\ \rho vY_k + \frac{1}{Re_{\delta_0}\ Sc}J_{k\,y} \end{pmatrix} \qquad (4, 5)$$

Here u and v represent streamwise and transversal velocities, ρ and P are the density and pressure of the system, Y_k is the mass fraction of the k^{th} chemical specie, with $k=0,..,.N$, where N is the number of chemical species in the reacting flow, E is the total energy of the system, Re_δ is the Reynolds number defined for δ_0, where δ_0 is the thickness of the mixing layer, Sc, Pr, Ec and Pe are the Schmidt, Prandtl, Eckert and Peclet numbers, $(\Delta x^*)_i$ and $(\Delta y^*)_j$ are the lengths of each spectral element in the directions x^* and y^*, respectively, The components of the mean strain tensor for a Newtonian fluid τ_{ij}, the components of the heat flux vector $\vec{q}$, and mass flux vector, $\vec{J}_k$ are defined by:

$$\tau_{xx} = (2\delta_0)\frac{2}{3}\mu\left(\frac{2}{(\Delta x^*)_i}\frac{\partial u}{\partial x} + \frac{1}{(\Delta y^*)_j}\frac{\partial v}{\partial y}\right),\ \tau_{yy} = (2\delta_0)\frac{2}{3}\mu\left(\frac{2}{(\Delta y^*)_j}\frac{\partial v}{\partial y} - \frac{1}{(\Delta x^*)_i}\frac{\partial u}{\partial x}\right) \quad (6, 7)$$

$$\tau_{xy} = (2\delta_0)\mu\left(\frac{1}{(\Delta x^*)_i}\frac{\partial u}{\partial x} + \frac{1}{(\Delta y^*)_j}\frac{\partial v}{\partial y}\right) \quad (8)$$

$$(q_c)_x = \left(\frac{1}{Ec}\right)\frac{2\delta_0}{(\Delta x^*)_i}k\frac{\partial\theta}{\partial x} + Le\sum_{k=1}^{N}h_k\rho(V_k)_x,\ (q_c)_y = \left(\frac{1}{Ec}\right)\frac{2\delta_0}{(\Delta y^*)_j}k\frac{\partial\theta}{\partial y} + Le\sum_{k=1}^{N}h_k\rho(V_k)_y \quad (9, 10)$$

$$\vec{J}_k = 2\delta_0\rho Y_k\vec{V}_k \quad (11)$$

Here h_k is the enthalpy of the k^{th} chemical species, and θ is the dimensionless temperature. The dimensionless diffusion velocity vector of the k^{th} species, $\vec{V}_k$ is:

$$(V_k)_x = -\frac{1}{X_k}D_{km}(d_k)_x - \frac{D_k^T}{\rho Y_k\theta}\frac{1}{(\Delta x^*)_i}\frac{\partial\theta}{\partial x},\ (V_k)_y = -\frac{1}{X_k}D_{km}(d_k)_y - \frac{D_k^T}{\rho Y_k\theta}\frac{1}{(\Delta y^*)_j}\frac{\partial\theta}{\partial y} \quad (12, 13)$$

$$(d_k)_x = \frac{1}{(\Delta x^*)_i}.\left(\frac{\partial X_k}{\partial x} + (X_k - Y_k)\frac{1}{P}\frac{\partial P}{\partial x}\right),\ (d_k)_y = \frac{1}{(\Delta y^*)_j}.\left(\frac{\partial X_k}{\partial y} + (X_k - Y_k)\frac{1}{P}\frac{\partial P}{\partial y}\right) \quad (14, 15)$$

D_k, D_k^T are the multi component diffusion and thermal coefficients, and X_k is the mole fraction of the k^{th} species. The temperature and pressure are calculated by the ideal gas equation.

2.1 The Initial Conditions

For the initial conditions, a one dimensional basic flow is imposed:

$$u^*(x, y, t = 0) = [U_o + U_1\tanh(y^*/\delta_0)] \quad (16)$$

$$v^*(x, y, t = 0) = 0 \quad (17)$$

$$T^*(x, y, t = 0) = [T_o + T_1\tanh(y^*/\delta_0)] \quad (18)$$

$$\rho^*(x, y, t = 0) = \lfloor f(T_\infty, Y_{k\infty}, P_\infty = 1atm.)\rfloor \quad (19)$$

$$Y_k(x, y, t = 0) = Y_{ko} + Y_{k1}\tanh(y^*/\delta_0) \quad (20)$$

Here the symbols ∞ and -∞ represent the air and hydrogen stream properties, and:

$$U_o = \frac{U_\infty + U_{-\infty}}{2},\ U_1 = \frac{U_\infty - U_{-\infty}}{2}, T_o = \frac{T_\infty + T_{-\infty}}{2},\ T_1 = \frac{T_\infty - T_{-\infty}}{2} \qquad (21, 22, 23, 24)$$

$$Y_{k\,o} = \frac{Y_{k\infty} + Y_{k-\infty}}{2},\ Y_{k1} = \frac{Y_{k\infty} - Y_{k-\infty}}{2} \qquad (25, 26)$$

2.2. The Boundary Conditions

Since the simulation has to account for spatial spreading, the boundary conditions at $x = -1$, i. e., downstream edge of the thin splitter plate, are of the Dirichlet type: the value of each variable is imposed, and one has one-dimensional basic flow perturbed by small random perturbation. At the end of domain, $x = 1$, Newman boundary conditions are applied. In the *y** direction, free-slip boundary conditions are chosen for $y = \pm 1$.

$$u^*(x = -1, y, t) = [\bar{u}(y^*) + f(y^*)\varepsilon\hat{V}(y^*, t^*)] \qquad (27)$$

$$v^*(x = -1, y, t) = [f(y^*)\varepsilon\hat{V}(y^*, t^*)] \qquad (28)$$

$$T(x = -1, y, t) = \left[T_o + T_1 \tanh(y^*/\delta_0)\right] \qquad (29)$$

$$\rho^*(x = -1, y, t = 0) = \left[f(T, Y_k, P_\infty)\right] \qquad (30)$$

$$Y_k(x = -1, y, t = 0) = Y_{k\,o} + Y_{k1} \tanh(y^*/\delta_0) \qquad (31)$$

$$\frac{\partial\varphi(x = 1, y, t)}{\partial x} = 0,\ \varphi = \{u, v, E, \rho, Y_k\} \qquad (32)$$

Here $\hat{V}(y^*, t^*)$ is a random number which constitutes a centered and reduced white noise perturbation. This white noise will inject the same small amount of energy into all the longitudinal modes of the basic flow. ε is the amplitude of the random perturbation. The function $f(y^*)$ represents a Gaussian filter modulating the amplitude of the perturbations, which confines all the perturbations of the basic flow to its rotational zone.

3. CHEMICAL SCHEME

The chemical kinetics used in the present study is given in Table 1. There are 19 chemical reactions and the chemical species considered are H_2, O_2, N_2, O, OH, H, H_2O, HO_2, H_2O_2. The rates of the chemical reactions and the thermodynamic and transport properties are calculated by the softwares Chemkin and Package for Evaluation of the Transport Properties, both developed by Sandia National Laboratories. The choice of the chemical scheme is somewhat arbitrary, no significant qualitative differences in the flow structure are observed using different chemical schemes.

Table 1. Gas Phase Mechanism of Hydrogen Oxidation, $k_{fi} = A_i (T)^{\beta_i} exp\left(- E_i / RcT \right)$.

Reaction	A (mol, cm, s)	β	E_i^* (Kcal/mol)
1. $O_2+H \Leftrightarrow O+OH$	1.92e14	0.0	16.44
2. $H_2+O \Leftrightarrow H+OH$	5.08e4	2.67	6.29
3. $H_2+OH \Leftrightarrow H_2O+H$	2.16e8	1.51	3.43
4. $OH+OH \Leftrightarrow H_20+O$	1.23e4	2.62	-1.88
5.[a] $H_2+M \Leftrightarrow H+H+M$	4.57e19	-1.4	104.4
6.[a] $O+O+M \Leftrightarrow O_2+M$	6.17e15	-0.50	0.0
7.[a] $O+H+M \Leftrightarrow OH+M$	4.72e18	-1.0	0.0
8.[a] $H+OH+M \Leftrightarrow H_2O+M$	2.25e22	-2.0	0.0
9.[a] $H+O_2+M \Leftrightarrow HO_2+M$	6.17e19	-1.42	0.0
10. $HO_2+H \Leftrightarrow H_2+O_2$	6.63e13	0.0	2.13
11. $HO_2+H \Leftrightarrow OH+OH$	1.69e14	0.0	0.87
12. $HO_2+O \Leftrightarrow OH+O_2$	1.81e13	0.0	-0.4
13. $HO_2+OH \Leftrightarrow H_20+O_2$	1.45e16	-1.0	0.0
14. $HO_2+HO2 \Leftrightarrow H_2O_2+O_2$	3.02e12	0.0	1.39
15.[a] $H_2O_2+M \Leftrightarrow OH+OH+M$	1.20e17	0.0	45.5
16. $H_2O_2+H \Leftrightarrow H_2O+OH$	1.00e13	0.0	3.59
17. $H_2O_2+H \Leftrightarrow H_2+HO_2$	4.82e13	0.0	7.95
18. $H_2O_2+O \Leftrightarrow OH+HO_2$	9.55e6	2.0	3.97
19. $H_2O_2+OH \Leftrightarrow H_2O+HO_2$	7.00e12	0.0	1.43

a – Third body enhancement: H_2O: 12; H_2: 25.

4. NUMERICAL METHOD

In this work the Collocation Spectral Elements Method with Chebyshev polynomials is used for spatial discretization of the partial differential equation system formed by the conservation equations. In most applications of spectral methods for the solution of partial differential equations, only the spatial discretization is spectral. In this case, to obtain a stable stationary solution, the spatial discretization is completely separated from the temporal discretization. First the discretization on spatial terms is done, an ordinary differential equation is obtained, where time is the only independent variable.

Considering the conservation equations in the vector form, given by Eq. (1), it is possible to define a function that characterizes the spectral projection in space, which is obtained from the calculation of the spatial derivative, as:

$$P(U_e) = -\frac{L_x}{(\Delta x^*)_i}\frac{\partial E}{\partial x} - \frac{L_x}{(\Delta y^*)_j}\frac{\partial F}{\partial y} + S \tag{33}$$

In this way, it is possible write the following ordinary differential equation:

$$\frac{d(U_e)}{dt} = P(U_e) \tag{34}$$

For the solution of the linear ordinary differential, Eq. (34), whose independent variable is the time a Runge-Kutta Method of order *s* is applied. This is a time-stepping procedure with multiple stages. All calculation were made using the Gauss-Lobatto collocation points, with a grid of 199x166. The physical domain length were established so that the lateral boundary conditions did not affect the development the mixing region necessary for the combustion processes. Also, the axial length was set up such as the reacting mechanisms attained a uniform spatial evolution. Normally, the structure of the spatial mixing layer for either reacting or homogenous flows depends significantly of the initial thickness vorticity. However, in this study one did not analyze the influence of this property. The results presented in this paper where obtained with δ_0=0.01m. The level of the random noise where set up with order 10^{-2}.

5. RESULTS

Figures (1a) and (1b) represent the temperature field for different dimensionless times, and Fig. (3c) the transversal velocity for an air stream which is at 5400m/s and 1200K and a slow fuel stream which is at 3000m/s and 500K; this is the Case 1. In a similar way, Fig. (2) represents an air stream which is at 1200K and 5400m/s and a fuel stream with 1200K and 3000m/s; this is the Case 2.

It is important to illustrate in a combustion problem both the flow dynamics and the combustion behaviors. The combustion is found to develop first on the air side of the mixing layer, as can be seen all graphics in Fig. (1) and (2). It is observed in Fig. (1c) and (2c) the transversal velocity evolution, that the flow is perturbed more intensely in a region in the fuel stream layer, with lower velocity than the stream oxidizer layer. This comportment flow is similar a region defined by a Mach cone with origin close to the trailing edge of the splitter plate.

One can observe in Fig. (1a) and (2a) for Cases 1 and 2, that for an early time where the mixing layer is not completely developed, that the level of temperature is not enough high. However, at a later time *t=1.800*, it is possible to observe different regions in the flow. First, there is an induction region, where the temperature remains quasi-constant. One can note that this region is smaller for Case 2. Later there is a thermal runaway region, which defines the induction length of the combustion process. This ignition point is located for Case 1 at *x*=-10cm* and *x*=-28cm* for Case 2. This shows that an efficient way to decrease the ignition distance is to increase the temperature of the fuel stream. In a similar way Figueira da Silva et al. (1993) have identified induction and thermal runway regions. In addition, they have identified a region where both premixed combustion and a diffusion flame coexist and a diffusion flame region. They have used classical boundary-layer equations, in steady state.

Figure (3) shows the mass fraction profile for Case 1. One can observe the excess of oxygen that is present in the H_2-air of the mixing layer, at a position after the ignition point. This fact characterizes a rich premixed H_2-air combustion zone. It should be noted that a similar structure is not found on the lean side of the mixing layer due to the large diffusion velocity of H_2. This result is consistent with that described by Figueira da Silva et al. (1993). This fact can be also observed for Case 2.

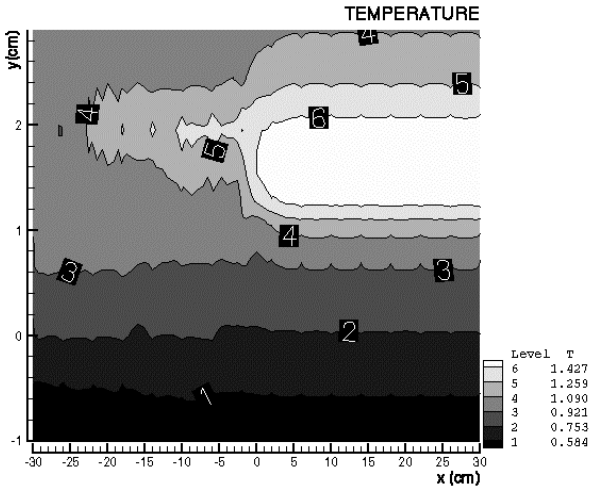

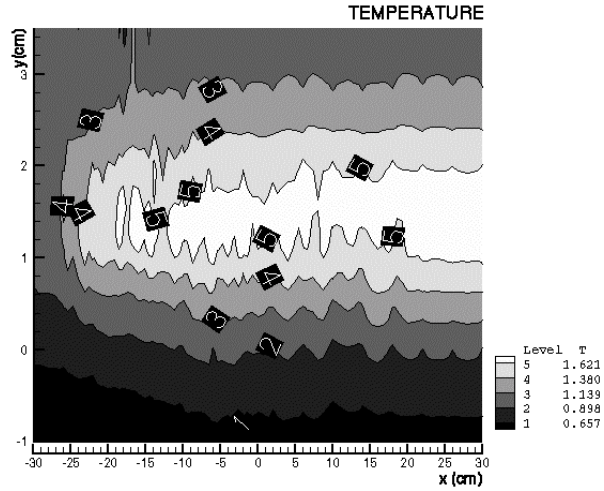

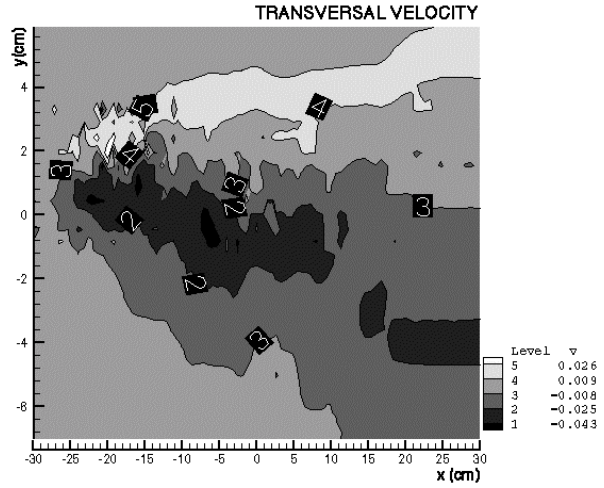

Figure 1. Case 1:
(a) Temperature field for *t=0.900.*
(b) Temperature field for *t=1.800.*
(c) Transversal Velocity field for *t=1.800.*

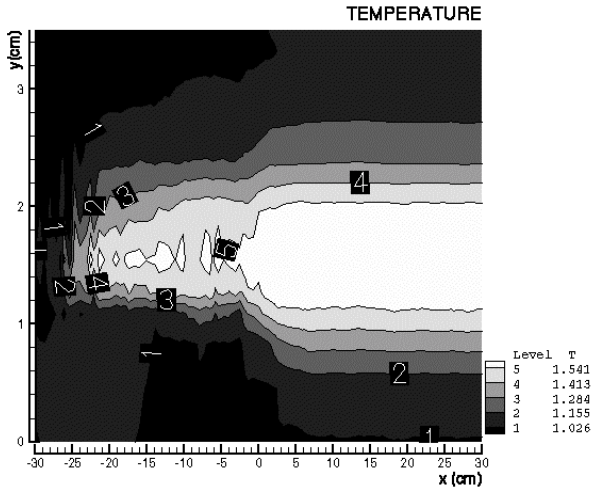

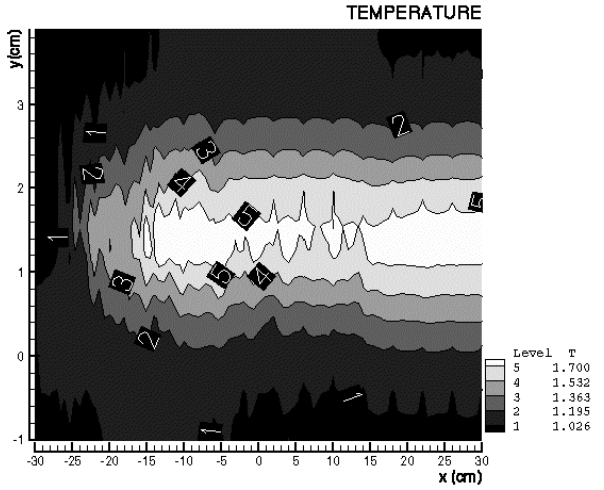

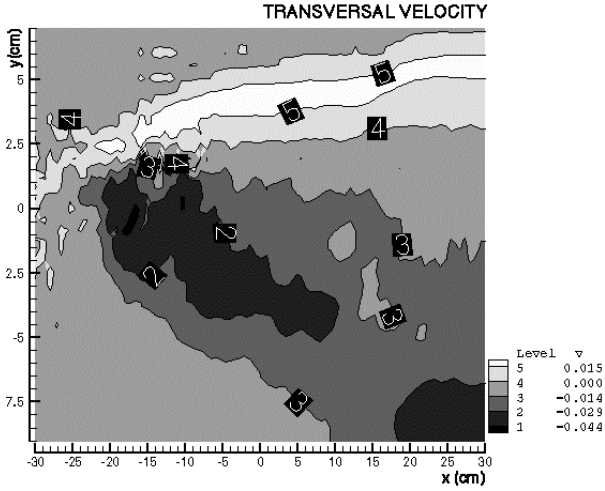

Figure 2. Case 2:
(a) Temperature field for *t=0.900.*
(b) Temperature field for *t=1.800.*
(c) Transversal Velocity field for *t=1.800.*

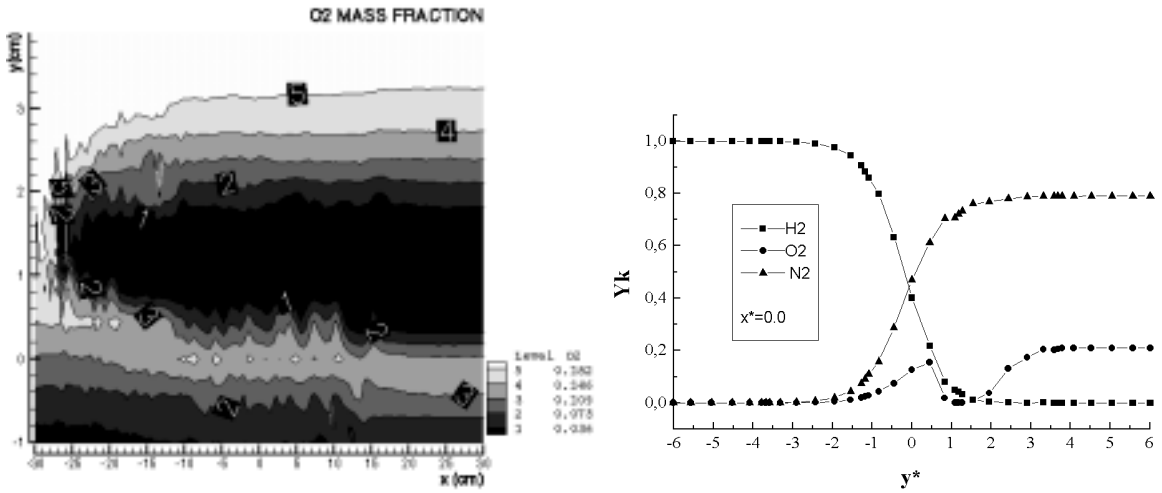

Figure 3. Case 1, for *t=1,800*: (a) O_2 mass fraction profile; (b) O_2, H_2 and N_2 mass fraction profiles.

Figure (4) represents the H_2O mass fraction profile for the two cases, while Fig. (5) and (6) show the mass fraction profiles for the major intermediate chemical species, *O, OH* and *H* for Case 1 and 2. The level of concentration of the species obtained in this work are almost the same as those obtained in Figueira da Silva et al. (1993) and Nishioka and Law (1995). It is important to note the similar aspect for the mass fraction profiles for the two cases.

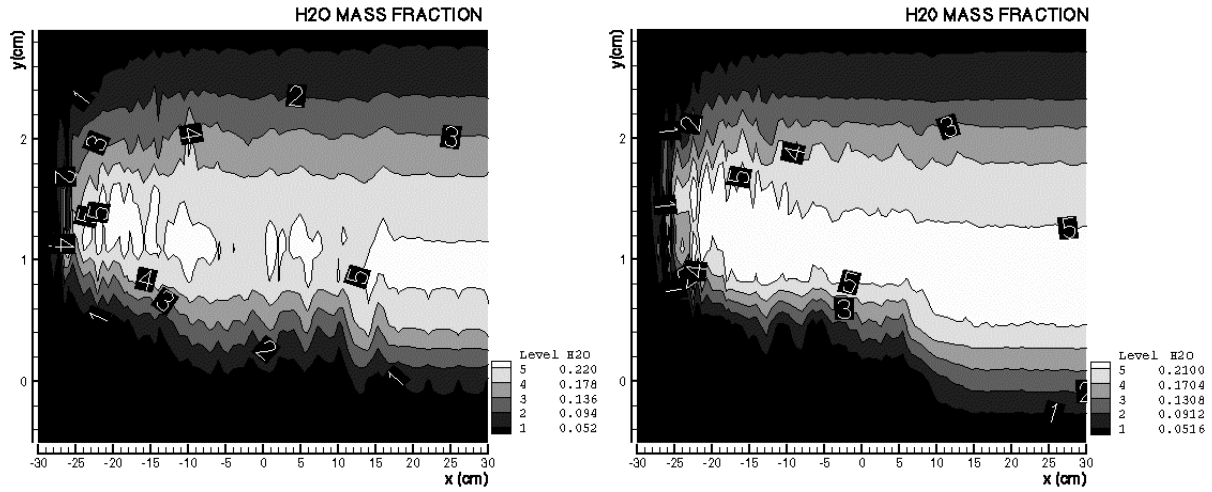

Figure 4. H_2O mass fraction profiles: (a) Case 1, for *t=1,800*; (b) Case 2, for *t=1,800*.

6. CONCLUSION

The basic structure of the combustion phenomena found in this work appears to be analogous to that described by Figueira da Silva et al. (1993) and Nishioka and Law (1995). However, more results for different stream conditions must be analyzed and analyzed statistically. For future work, it is important to verify the dependence of ignition distance on the various system parameters like Mach, Reynolds and Eckert numbers, temperature of fuel and oxidizer, and pressure.

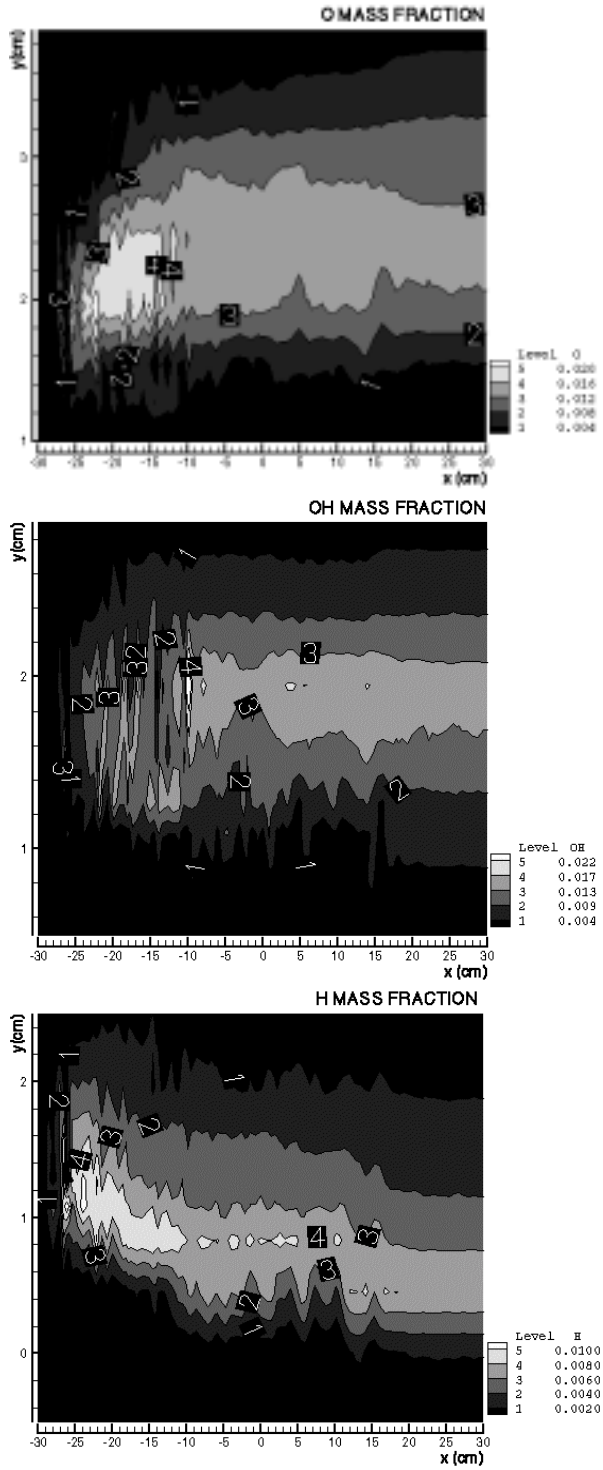

Figure 5. Case 1, mass fraction profiles: for *t=1,800*, a) *O*, b) *OH*, c) *H*.

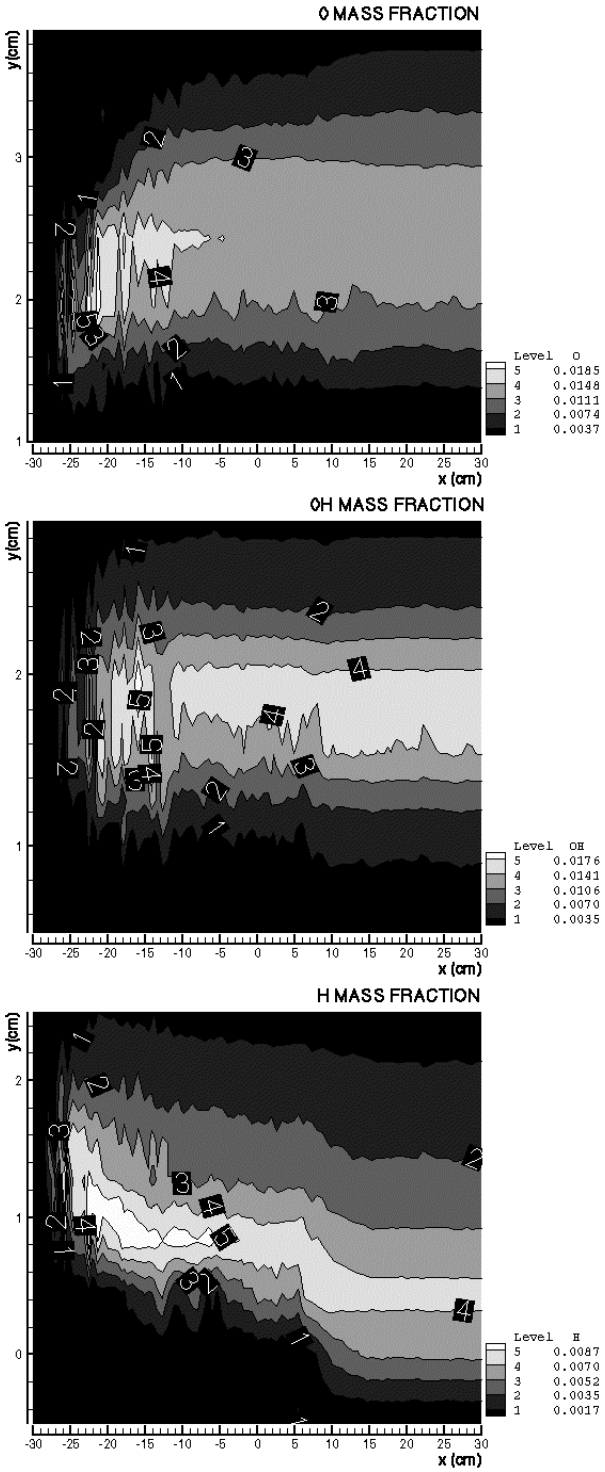

Figure 6. Case 1, mass fraction profiles: for *t=1,800*, a) *O*, b) *OH*, c) *H*.

7. REFERENCES

Faria, A. F. et al. (1998), Simulation of ignition in supersonic H_2-air unsteady mixing layer using spectral method. *VII ENCIT*, Rio de Janeiro. Brazil,1, 126-131.

Faria, A. F. et al. (1999), Numerical investigation upon the No formation in the H2-air ignition in the supersonic unsteady mixing layer. *XV COBEM*, Águas de Lindóia, Brazil.

Faria, A. F. et al. (1999), Collocation spectral elements method for simulation of reactive mixing layer. *XX CILANCE*, São Paulo, Brazil.

Canuto, C. et al. (1988), *Spectral methods in fluid dynamics*. Springer-Verlag (1988).

Figueira da Silva, L. F. et al. (1993); Some specific aspects of combustion in supersonic H_2-air laminar mixing layers. *Combustion Science and Technology*, 89, 317-333.

Nishioka, M. and Law, C. K. (1995); A numerical study of ignition in the supersonic hydrogen/air laminar mixing layer. *AIAA* Paper 95-0377.

Comte, P. et al. (1989), Numerical simulations of turbulent plane shear layers. *Turbulent Shear Flow*, 6, 360-380.

Kee, R. J. et al. (1989); Chemkin-II: A Fortran chemical kinetics package. *Sandia Report*, Sand89-8009b Uc706.